

# Dedicated Cutback Control of a Wind Power Plant Based on the Ratio of Command Power to Available Power

Khagendra Thapa\*, Gihwan Yoon\*, Sang Ho Lee\*\*, Yongsug Suh\*\*\*  
and Yong Cheol Kang<sup>†</sup>

**Abstract** – Cutback control in a grid code is one of the functions of a wind power plant (WPP) that is required to support the system protection and frequency stability. When a cutback control command signal is delivered to the WPP from the system operator, the output of a WPP should be decreased to 20% of the rated power within 5 s. In this paper, we propose a dedicated cutback control algorithm of a WPP based on the ratio of the command power to the available power. If a cutback control signal is delivered, the algorithm determines the pitch angle for the cutback control and starts the pitch angle control. The proposed algorithm keeps the rotor speed at the speed before the start of the cutback control to quickly recover the previous output prior to the cutback control. The performance of the algorithm was validated for a 100 MW aggregated WPP based on a permanent magnet synchronous generator under various wind conditions using an EMTP-RV simulator. The results clearly shows that the proposed algorithm not only successfully reduces the output to the command power within 5 s by minimizing the fluctuation of the pitch angle, but also rapidly recovers to the output level before the cutback control.

**Keywords:** Cutback control, Pitch angle control, Power coefficient, Rotor speed, Wind power plant

## 1. Introduction

Generation in a power system should be balanced with the consumption to keep the frequency within the allowed limit at all times. Stability problems in terms of the frequency will occur if a severe mismatch between generation and consumption happens in a power system. Power plants should regulate their production to match the demand in order to avoid long term unbalanced conditions in a power system [1].

Wind generation has rapidly increased due to technological advances and economic viability over the decades. The total worldwide installed wind generation capacity increased to 199 GW in 2010 and is expected to increase to 832 GW by 2020 and 3,702 GW by 2050 [2]. In Korea, a 2.5 GW offshore wind power plant (WPP) project on the southwestern coast was started in 2011 [3].

Due to the inherent intermittency and volatility of wind, high wind penetration raises a challenge to the frequency stability in a power system. Therefore, a grid code specifies that a large scaled WPP is required to have the capability to

regulate their active and reactive power in order to minimize the effects of variable wind generation on the stability of a power system. A grid code typically includes the active power/frequency control, reactive power/voltage control, and fault ride-through capability [4, 5].

Variable speed wind generators (VSWGs), such as doubly-fed induction generators (DFIGs) and permanent magnet synchronous generators (PMSGs), have been widely used to achieve a maximum power point tracking (MPPT) control mode below the rated wind speed. Above the rated wind speed, they control the output power by adjusting the pitch angle depending on the de-loaded power.

The active power control requirements in a grid code can be divided into absolute power control, delta control, balance control, ramp limitation, and fast down regulation control [6, 7]. Among these, the fast down regulation is also known as the cutback power control, which requires a WPP to reduce the output power to 20% of its rated power within 5 s. The cutback control is required to very rapidly regulate the output of a WPP to support the frequency stability and system security [8, 9].

Up until this point, dedicated cutback control has not yet been suggested. Some pitch control methods to regulate the output power have been proposed [10, 11]. A pitch control algorithm is activated based on the wind speed, the rotor speed, and the output power [10]. A pitch control of the DFIG-based WPP has been suggested in order to regulate the output power to the reference power ordered by the system operator [11]. The algorithm activates the pitch control only when the rotor speed exceeds the threshold

<sup>†</sup> Corresponding Author: Dept. of Electrical Engineering, WeGAT Research Center, and Smart Grid Research Center, Chonbuk National University, Korea. (yckang@jbnu.ac.kr)

\* Dept. of Electrical Engineering and WeGAT Research Center, Chonbuk National University, Korea. ({khagen, kihwan01}@jbnu.ac.kr)

\*\* Korea Electro technology Research Institute, Korea (sanghlee@keri.re.kr).

\*\*\* Dept. of Electrical Engineering, WeGAT Research Center, and Smart Grid Research Center, Chonbuk National University, Korea. (ysuh@jbnu.ac.kr)

Received: February 22, 2014; Accepted: March 15, 2014

value, which is slightly less than the maximum operating limit of the rotor speed. However, this might cause a significant fluctuation in the pitch angle during the cutback control.

In this paper, we propose a dedicated WPP cutback control algorithm that employs the pitch control based on the ratio of the command power to the available power. If a cutback control signal is delivered from the system operator, then the algorithm determines the pitch angle to conduct the cutback control and starts the pitch angle control. The proposed algorithm keeps the rotor speed the same as that before the start of the cutback control to minimize the fluctuation of the pitch angle and recover the output of the WPP to its previous value within a short time interval. The performance of the algorithm was validated for a 100 MW aggregated PMSG-based WPP under various wind conditions using an EMT-P-RV simulator.

## 2. Dedicated Cutback Control for a PMSG-based WPP

The goal of this paper is to design a dedicated cutback control algorithm of a PMSG-based WPP that regulates the output power to 20% of the rated power within 5 s by reducing the fluctuation of the pitch angle, and rapidly recovers to the pre-cutback control value once the cutback command signal is disabled. In order to achieve this, the algorithm determines the pitch angle based on the command power and the available power.

For convenience, we assumed a PMSG-based WPP as a single PMSG with a fully rated converter (FRC) as shown in Fig. 1 in this paper. The PMSG consists of back-to-back voltage source converters. The machine side converter (MSC) shown in Fig. 1 controls the output of the PMSG while a grid side converter (GSC) controls the dc link voltage and the grid voltage. In this paper, we assumed that the WPP is operating in the MPPT control mode before the cutback control mode. In the next two sections, we will describe the two control modes of operation of the MSC, i.e., the MPPT mode and the cutback control mode.

### 2.1 MPPT control mode

The available power in the wind ( $P_{air}$ ) can be expressed by

$$P_{air} = 0.5\rho Av^3 \quad (1)$$

where  $\rho$  is the air density,  $A$  is the area swept by the blades, and  $v$  is the wind speed.

The mechanical input power ( $P_{mech}$ ) is given by

$$P_{mech} = 0.5\rho Ac_p(\lambda, \beta)v^3 \quad (2)$$

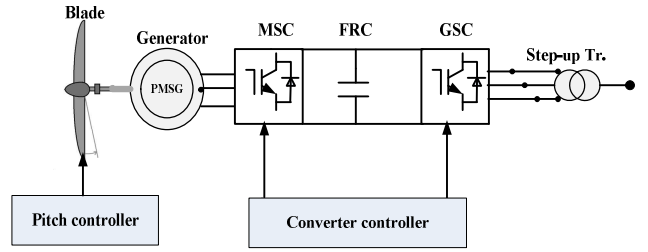


Fig. 1. PMSG configuration

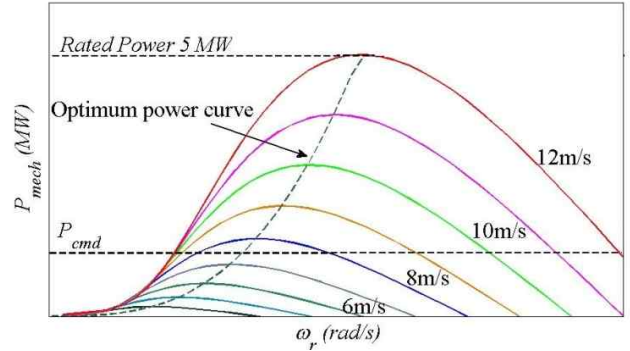


Fig. 2. Characteristics curve for the power and rotor speed with the command power

where  $c_p$  is the power coefficient of the WG (unitless) that is the function of the tip speed ratio ( $\lambda$ ) and the blade pitch angle ( $\beta$ ) in deg.

$\lambda$  is defined as:

$$\lambda = \frac{\omega_r R}{v} \quad (3)$$

where  $\omega_r$  and  $R$  are the turbine rotor speed in rad/s and the rotor radius in m, respectively.

In order to extract the maximum power from the wind,  $c_p$  should be at its maximum. To achieve this,  $\lambda$  was kept constant at its optimum value. Fig. 2 shows the maximum power in the MPPT mode [12], which can be expressed by

$$P_{max} = k_{opt} \omega_{opt}^3 \quad (4)$$

where  $\omega_{opt}$  is the optimum rotor speed and  $k_{opt}$  is the constant.

The reference of the MSC for the MPPT control  $P_{ref}$  was set to

$$P_{ref} = k_g \omega_r^3 \quad (5)$$

where  $k_g$  is a function of the parameters such as the gear-ratio, blade length, and blade profile, etc.

### 2.2. Proposed cutback control mode

Fig. 3 shows a schematic diagram of the proposed

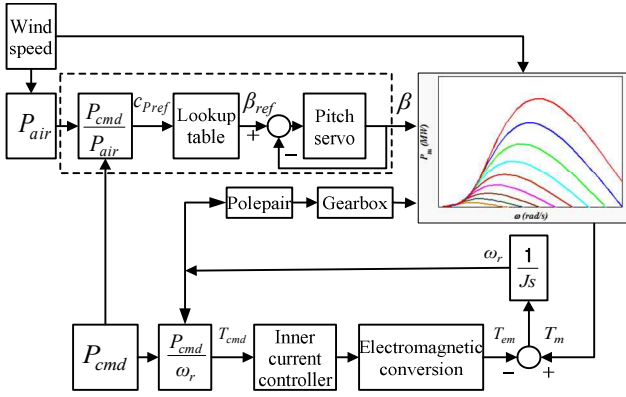


Fig. 3 Schematic diagram of the proposed control strategy

control strategy for the PMSG. If the command power ( $P_{cmd}$ ) is dispatched to the WPP, then the output power should be rapidly reduced from  $P_{max}$  to  $P_{cmd}$ . This result indicates the mode changes from the MPPT mode to the cutback control mode. The torque command ( $T_{cmd}$ ) is obtained by dividing  $P_{cmd}$  by  $\omega_r$  and used to obtain the direct axis current ( $I_d$ ). With a proper reference frame arrangement,  $I_d$  is used to obtain the electromagnetic torque ( $T_{em}$ ). If  $P_{cmd}$  is applied to the PMSG, then the mechanical power might not be equal to  $P_{cmd}$ . Consequently, the rotor speed would accelerate or decelerate depending on the difference between the  $T_{mech}$  and  $T_{em}$  as shown by

$$T_{mech} - T_{em} = J \frac{d\omega_r}{dt} \quad (6)$$

where  $J$  is the inertia of a motion system.

The change in the  $\omega_r$  affects  $\lambda$  and, therefore, changes  $c_p$ . As a result,  $P_{mech}$  changes [13]. The proposed algorithm remains at  $\lambda$  as the previous constant value. Therefore,  $c_p$  only depends on the pitch angle. Therefore, the proposed algorithm controls  $P_m$  by controlling the pitch angle based on the ratio of  $P_{cmd}$  to  $P_{air}$ , i.e.,

$$c_{Pref} = \frac{P_{cmd}}{P_{air}} \quad (7)$$

Fig. 4 shows the relationship between the  $c_p$  and  $\lambda$  with the pitch angle. The vertical dotted line in Fig. 4 indicates a constant  $\lambda$  of 9.95 as an example. Similarly, the horizontal dotted line represents the reference power coefficient ( $c_{Pref}$ ), which is calculated by using (7). Then, the reference pitch angle ( $\beta_{ref}$ ) for the  $c_{Pref}$  can be obtained. In this way, the pairs of  $\beta_{ref}$  and  $c_{Pref}$  can be obtained and are represented in the graph as shown in Fig. 5.

The proposed algorithm made a group of the graphs depending on the different  $\lambda$  in the lookup table. If  $c_{Pref}$  decreased, then the  $\beta_{ref}$  increased as shown in Fig. 5.

Fig. 6 shows the logic behind the pitch angle controller.  $\beta_{ref}$ , which was obtained from the lookup table, is used as an input for the pitch servo controller with a feedback

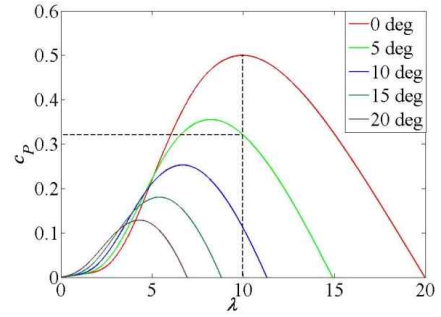


Fig. 4.  $C_p$ -  $\lambda$  characteristics curves with a pitch angle

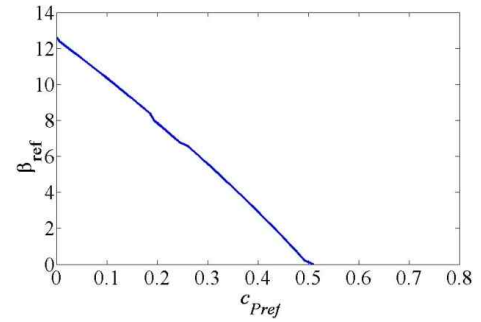


Fig. 5.  $\beta_{ref}$  vs  $c_{Pref}$  curve for a tip speed ratio of 9.95

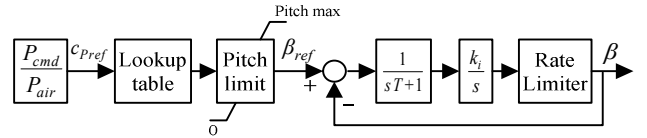


Fig. 6. Proposed pitch angle controller

loop. The pitch servo consists of the low pass filter, the integrator, and the rate limiter. The integrator is used as an actuator of the pitch angle controller and produces  $\beta$ . The time constant of the pitch servo ( $T_s$ ), which depends on the type and capacity of the WG, was set to 1 s for 5 MW WG in this study [14]. The rate limiter restricts the maximum rate of change of the pitch angle depending on the size of the WG. The range of the rate limiter is known as 3-10 deg/s [8] or 5-10 deg/s [15]. In this study, 10 deg/s was used as the maximum rate of change of the pitch angle.

### 3. Model System

In order to investigate the performance of the cutback control algorithms for the aggregated WPP, the model system shown in Fig. 7 was chosen. The system consists of a 100 MW aggregated WPP, five synchronous generators (SGs) (two 200 MVA SGs, two 150 MVA SGs, and one 100 MVA SG), and a load of 600 MW and 9 MVar.

The WPP was represented by an aggregated PMSG with an FRC.  $P_{cmd}$  was set to 20% of the rated capacity of the WPP. The generation voltage of the WG was 2.31 kV and the WG is connected to a feeder cable through a 2.31/33 kV step-up transformer. The cable is connected to the two

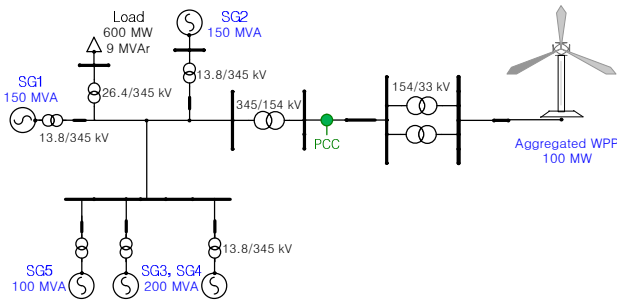


Fig. 7. Model system configuration

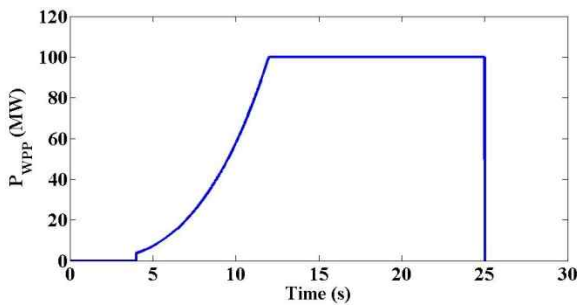


Fig. 8. Power curve of a 100 MW aggregated WPP

Table 1. Values of the parameters

Parameters	Values
WG rated capacity $P$ (MW)	5
Rotor radius $R$ (m)	54.9
Maximum Power coefficient $c_{p_{max}}$	0.5
Air density $\rho$ ( $\text{kg/m}^3$ )	1.225
Number of pole pairs $np$	200
Rated voltage $V$ (kV)	2.31
DC link voltage $V_{dc}$ (kV)	6.4
Inertia of turbine $H_t$ (s)	4
Inertia of generator $H_g$ (s)	1
Frequency $f$ (Hz)	60
Pitch angle rate limiter $d\beta/dt$ (deg/s)	10
Integral gain $K_i$	10

33/154 kV substation transformers. The rating of each transformer is 60 MVA. A substation is connected to the on-shore grid through a 22 km submarine intertie cable.

Fig. 8 depicts the power curve of a 100 MW aggregated WPP model based on a PMSG, where the cut-in, rated, and cut-out wind speeds are 4 m/s, 12 m/s, and 25 m/s, respectively. Table 1 shows the values for the parameters used in the case studies.

#### 4. Case Studies

The performance of the proposed algorithm was validated by comparing its result with the conventional algorithm in [11] with the wind speeds of 12 m/s, 10 m/s, and varying wind speed. Figs. 9(a)-11(a), Figs. 9(b)-11(b), and Figs. 9(c)-11(c) show the active power of the WPP, the pitch angle of the WG, and the rotor speed of the WG,

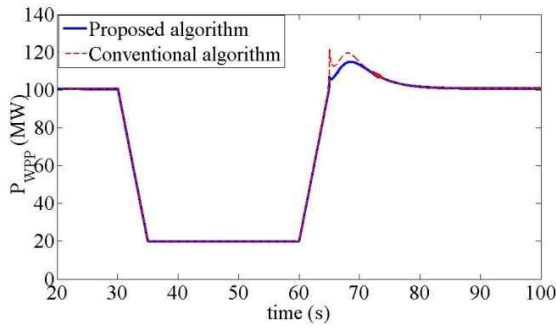
respectively. The thick and dotted lines represent the results of the proposed and conventional algorithms, respectively. We assumed that the cutback control to 20% of the rated power (20 MW) was delivered at 30 s for all the cases and disabled at 60 s for the cases of 1 and 2. For case 3, it was disabled at 155 s.

##### 4.1 Case 1: Wind speed of 12 m/s

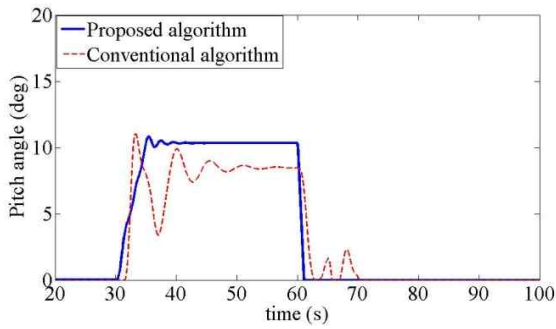
Fig. 9 shows the results for case 1, which is the rated wind speed. As shown in Fig. 9(a), both the proposed and conventional cutback control algorithms are operating in the MPPT mode, generating the maximum output power of 100 MW before the cutback control. If a cutback command signal is delivered at 30 s, both of the algorithms start reducing the output with the down ratio of the difference between the current power and command power to the time period of 5 s. Therefore, the output power of the WPP successfully reaches the command power of 20 MW at 35 s. During this time period, the pitch angle and rotor speed increase as shown in Figs. 9(b) and 9(c). When the cutback command is disabled at 60 s, then the output reference for increasing is set to the same ratio as the down ratio for 5 s in this study, and the pitch angle decreases with the pitch angle speed limitation of 10 deg/s. We see a larger overshoot in the conventional algorithm than in the proposed algorithm when a cutback command is completely deactivated at 65 s. This is because the rotor speed at 65 s is greater than that of the proposed algorithm.

The proposed algorithm determines the reference value of  $c_p$  of 0.099 using (7) and then the corresponding reference pitch angle of 10.3 deg from the lookup tables relating the reference to the power coefficient. The proposed algorithm starts the pitch control at 30 s, while the conventional algorithm starts it at 31.5 s, where the rotor speed reaches the threshold value of 1.2 pu. This is because the pitch control of the conventional algorithm is only activated when the rotor speed exceeds the threshold. For the conventional algorithm, the pitch angle reaches the peak value of 11.1 deg at 33.4 s and repeats the fluctuation until it reaches an equilibrium value of 8.5 deg. For the proposed algorithm, the pitch angle reaches the peak value of 10.8 deg at 35.5 s. The fluctuation of the pitch angle in the proposed algorithm is very small, while the fluctuation of the conventional algorithm is significant. In addition, the pitch angle for the proposed algorithm converges faster than that of the conventional algorithm. Moreover, we can see a large fluctuation in the pitch angle even after deactivation of the cutback control in the case of the conventional algorithm. The pitch angle of the proposed algorithm reaches zero at 61.1 s after the deactivation of the cutback control at 60 s.

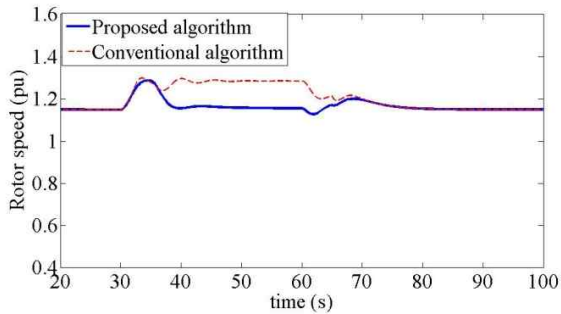
The rotor speed in the MPPT mode is 1.15 pu for both of the control algorithms as shown in Fig. 9(c). For the conventional algorithm, the rotor speed starts increasing at 31.5 s and reaches its peak value of 1.30 pu at 33.6 s. The



(a) Active power of the WPP

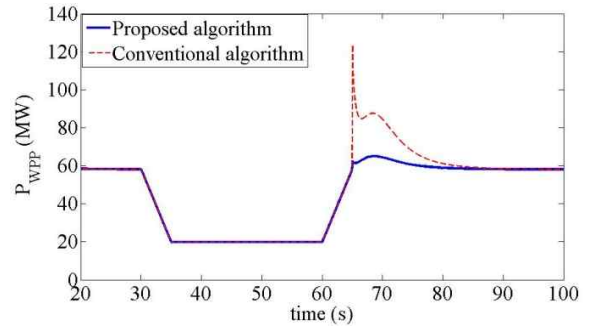


(b) Pitch angle of the WG

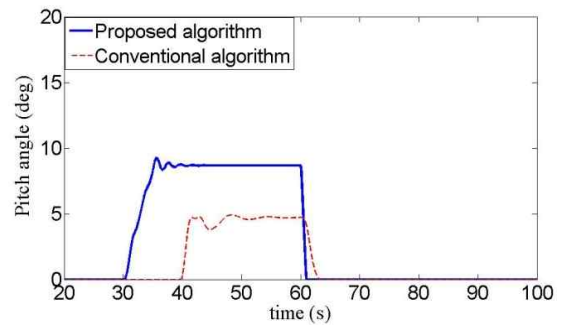


(c) Rotor speed of the WG

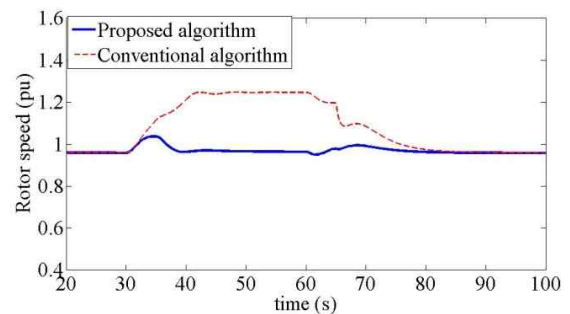
**Fig. 9.** Results for case 1



(a) Active power of the WPP



(b) Pitch angle of the WG



(c) Rotor speed of the WG

**Fig. 10.** Results for case 2

rotor speed keeps fluctuating until it reaches an equilibrium rotor speed of 1.28 pu. The difference between the two rotor speeds is 0.13 pu during the cutback control mode. For the proposed algorithm, the rotor speed increases and reaches 1.29 pu at 34.5 s. Then, it decreases to 1.16 pu at 39.9 s and remains at this value until the cutback signal is disabled. This result indicates that the proposed algorithm keeps the rotor speed at a value similar to 1.15 pu. The maximum operating limit of the rotor speed of the WG was set to 1.3 pu in this study. After the deactivation of the cutback control, the rotor speeds successfully returns to 1.15 pu for both of the algorithms.

#### 4.2 Case 2: Wind speed of 10 m/s

Fig. 10 shows the results for case 2. The output power of the WPP in the MPPT mode is 58.53 MW. The output

power reduces to the command power (20 MW) within 5 s as shown in Fig. 10(a). After deactivation of the cutback control at 60 s, the output power of the WPP for the proposed algorithm reaches its previous output power (58.53 MW) with a small overshoot within a short time, while the output power for the conventional algorithm returns to the previous value with a large overshoot, which exceeds the rated capacity of the WPP.

The proposed algorithm determines the reference value of  $c_p$  to be 0.173 using (7) and then the corresponding reference pitch angle was determined to be 8.7 deg from the lookup table. The proposed algorithm starts the pitch control at 30 s, while the conventional algorithm starts it at 39.6 s. For the conventional algorithm, the pitch angle reaches the peak value of 4.9 deg at 48.3 s and repeats fluctuation until it reaches an equilibrium value of 4.7 deg. Meanwhile, the pitch angle reaches the peak value of 9.2

deg at 35.7 s for the proposed algorithm. As in case 1, the fluctuation of the pitch angle in the proposed algorithm is minimal, while the fluctuation of the conventional algorithm is significant. In addition, the pitch angle for the proposed algorithm converges much faster than that of the conventional algorithm. The pitch angle of the proposed algorithm reaches zero at 60.9 s after the deactivation of the cutback control.

The optimum rotor speed in the MPPT mode for both of the algorithms is 0.96 pu. During the cutback control, the rotor speed of the conventional algorithm increases and reaches its peak value of 1.25 pu at 42.3 s and maintains this value. The difference between the two rotor speeds is 0.29 pu, which is more than twice the difference in case 1. For the proposed algorithm, the rotor speed increases and reaches the peak value of 1.04 pu at 34.6 s. Then, it decreases to 0.96 pu at 38.5 s, which is the same as the value in the MPPT mode, and it is maintained at this value until the cutback signal is disabled. After the deactivation of the cutback control, the rotor speeds successfully returns to 0.96 pu for both of the algorithms. However, the conventional algorithm needs more time to reach the value.

### 4.3 Case 3: Varying wind speed

Fig. 11 shows the results for case 3, which is identical to case 1 except that the wind speed changes from 12 m/s to 10 m/s at 55 s and from 10 m/s to 12 m/s at 135s. The results in case 3 are the exactly the same as in case 1 before the wind speed changes from 12 m/s to 10 m/s.

After deactivation of the cutback control at 155 s, the output power of the WPP for both of the algorithms successfully reaches its previous output power (100 MW). We see a larger overshoot in the conventional algorithm than in the proposed algorithm when a cutback command is completely deactivated. This is because the rotor speed at 155 s is greater than that of the proposed algorithm as in case 1. The proposed algorithm determines that the reference value of  $c_p$  is 0.099 and 0.173 using (7) for 12 m/s and 10 m/s, respectively.

The corresponding reference pitch angles are 10.3 deg and 8.7 deg, respectively. When the wind speed changes from 12 m/s to 10 m/s, the pitch angle of the conventional algorithm decreases before converging of the pitch angle and reaches 4.8 deg at 62.3 s, and stays an equilibrium value of 4.7 deg at 72.5 s until the wind speed changes. Similarly, for the proposed algorithm, the pitch angle starts decreasing at 55 s and reached at 8.5 deg at 71.2 s with a very small ripple. When the wind speed changes from 10 m/s to 12 m/s, the proposed algorithm reaches an equilibrium value faster than the conventional algorithm with a negligible ripple. As in case 1, after the activation of the cutback control, the pitch angle reached zero faster than the conventional algorithm with a negligible ripple.

When the wind speed changes from 12 m/s to 10 m/s, for the conventional algorithm, the rotor speed reaches an equilibrium value of 1.25 pu at 61.6 s. In addition, when the wind speed changes from 10 m/s to 12 m/s, the rotor speed reaches an equilibrium value of 1.28 pu at 142.2 s. For the proposed algorithm, the tip speed ratio of the WG

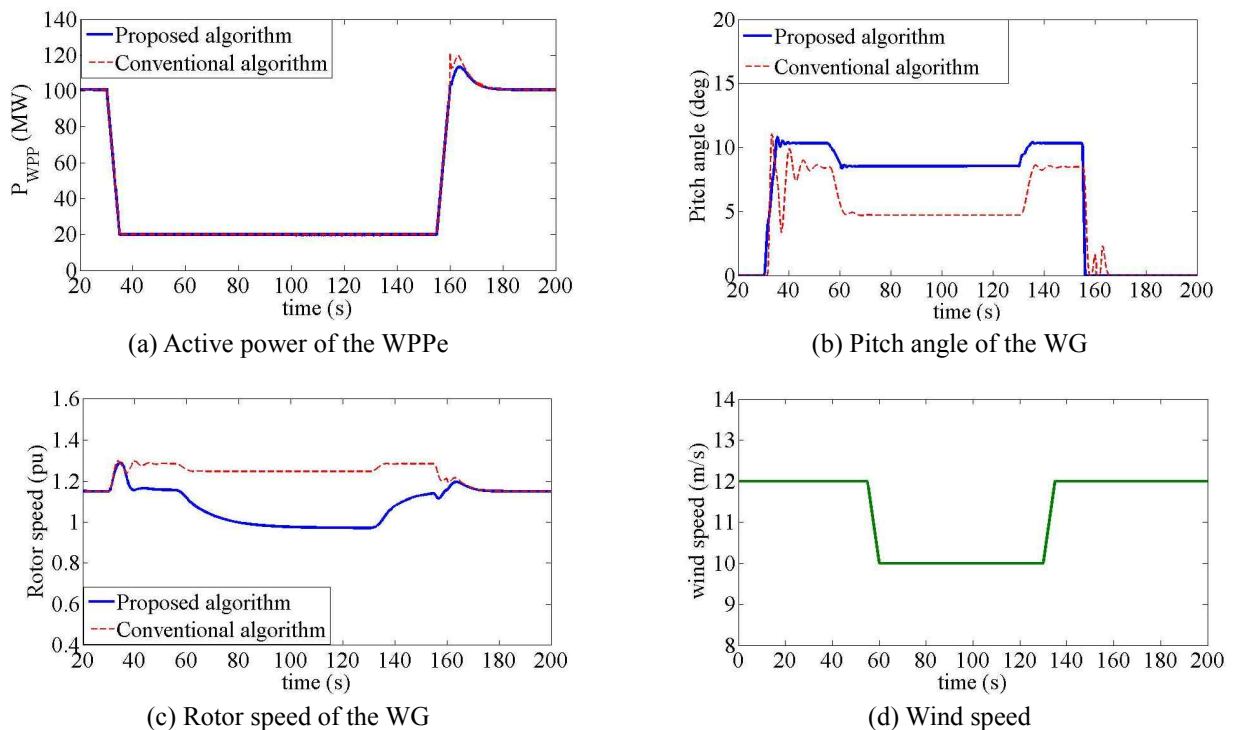


Fig. 11. Results for case 3

increases because of the reduction of the wind speed. In order to keep the tip speed ratio at 9.95, the algorithm starts decreasing the tip speed ratio and converges at 0.96 pu at 105.9 s. Similarly, the rotor speed starts increasing again after the wind speed changes from 10 m/s to 12 m/s. Note that cutback control is disabled before the rotor speed reaches an equilibrium point for the proposed algorithm. However, the algorithm successfully returns to 1.15 pu as in the conventional algorithm.

## 5. Conclusions

In this paper, we propose an algorithm for the dedicated cutback power control of the PMSG-based WPP that employs the pitch control based on the ratio of the command power to the available power. In order to reduce the output to the required value within 5 s, when a cutback control signal is delivered, the algorithm determines the power coefficient required to satisfy the command power and the corresponding pitch angle. Then, the algorithm controls the pitch angle with the pitch speed limitation of 10 deg/s immediately after the command was delivered.

The performance of the algorithm was investigated for the 100 MW PMSG-based WPP under various wind conditions. The results clearly shows that the algorithm successfully reduces the output to the command power within the specified time, and also recovers to the output level before the cutback control within a short time interval.

The advantages of the proposed algorithm lie in the fact that the rotor speed can be kept at the speed before the start of the cutback control and, therefore, the fluctuation of the pitch angle can be minimized during and after the cutback control.

## Acknowledgements

This work was supported by the National Research Foundation of Korea (NRF) grant funded by the Korea government (MSIP) (No. 2010-0028509) and KESRI (No. 2009T100100597) funded by MKE (Ministry of Knowledge Economy).

## References

- [1] J. Machowski, J.W. Bialek, and J.R. Bumby, *Power System Dynamics: Stability and Control*, 2nd Edition, United Kingdom, John Wiley & Sons, Ltd, 2008.
- [2] *Global wind energy outlook 2010*, Global Wind Energy Council, Oct. 2010.
- [3] *Global Wind Energy Report: Annual market update 2011*, Global Wind Energy Council, Mar. 2012.
- [4] M. Tsili, C. Patsiouras, and S. Papathanassiou, "Grid code requirements for large wind farms: A review of technical regulations and available wind turbine technologies," *Euro. Wind. Energy. Conference Expo*. 2008, pp. 1-11.
- [5] E. Fagan, S. Grimes, J. McArdle, P. Smith, and M. Stronge, "Grid code provisions for wind generators in Ireland," *IEEE conference on Power Engineering Society General Meeting*, 2005, vol. 2, pp. 1241-1247.
- [6] P. Sorensen, A. D. Hansen, F. Iov, F. Blaabjerg, and M.H. Donovan, "Wind farm models and control strategies," Riso National Laboratory, Roskilde, Denmark, 2005.
- [7] Nordic Grid code 2007.
- [8] T. Ackermann, *Wind Power in Power System*, 2nd Edition, England, John Wiley & Sons, Ltd, 2012.
- [9] A. D. Margaris, A. D. Hansen, P. Sorensen, and N. K. Hatziaargyriou, "Illustration of modern wind turbine ancillary services," *Energies*, vol. 3, 2010 pp. 1290-1302.
- [10] J. Zhang, M. Cheng, Z. Chen, and X. Fu, "Pitch angle control of variable speed wind turbines," *IEEE Conference on Electric Utility Deregulation and Restructuring and Power Technologies*, 2008, pp. 2691-2696.
- [11] C.C. Le-Ren, and Y. Yao-Ching, "Strategies for operating wind power in a similar manner of conventional power plant," *IEEE Trans. on Energy Conversion*, vol. 24, no. 4, 2009, pp. 926-934.
- [12] S. Morimoto, H. Nakayama, M. Sanada, and Y. Takeda, "Sensorless output maximization control for variable speed wind generation system using IPMSG," *IEEE Trans. on Industry Applications*, vol. 41, no. 1, 2005, pp. 60-67.
- [13] J. L. Rodriguez-Amenedo, S. Arnalte, and J. C. Burgos, "Automatic generation control of a wind farm with variable speed wind turbines," *IEEE Trans. on Energy Conversion*, vol. 17, no. 2, pp. 279-284, 2002.
- [14] A. Hwas and R. Kattebi, "Wind turbine control using PI pitch angle controller," *IFAC Conference on Advances in PID control*, Mar. 28-30, 2012.
- [15] S. Heier, *Grid integration of wind energy conversion systems*, United Kingdom, John Wiley & Sons, Ltd, 2nd Edition, 2006.



**Khagendra Thapa** He received his B. S. degree from Tribhuvan University, Nepal, in 2009. He is currently pursuing his M. S. degree at Chonbuk National University. He is also an assistant researcher at the Wind energy Grid-Adaptive Technology (WeGAT) Research Center supported by the Ministry of Science, ICT, and Future Planning (MSIP), Korea. His research interests include control and protection systems for wind power plants.



**Gihwan Yoon** He received his B.S. degree from Chonbuk National University, Korea, in 2013. He is currently pursuing his M.S. degree at Chonbuk National University. He is also an assistant researcher at the WeGAT supported by the MSIP, Korea. His research interests include development of wind energy grid integration techniques.



**Sang Ho Lee** He received his B.S., M.S., and Ph.D. degrees from Seoul National University, Korea, in 1995, 1997, and 2003, respectively. He has been with Korea Electro technology Research Institute (KERI), Korea, since 2003. He is currently a senior researcher at KERI, Korea. His research interests include the development of an energy management system for power systems and wind farms as well as optimal operating schemes for the smart grid.



**Yongsug Suh** He received B.S. and M.S. in Electrical Engineering from Yonsei University, Seoul, Korea, in 1991 and 1993, respectively, and his Ph.D. in Electrical Engineering from the University of Wisconsin, Madison, WI, USA, in 2004. Since 2008, he has been with the Department of Electrical Engineering, Chonbuk National University, Jeonju, Korea, where he is currently an Associate Professor. His current research interests include the power conversion systems of high power for renewable energy sources and medium voltage electric drive systems.



**Yong Cheol Kang** He received his B.S., M.S., and Ph.D. degrees from Seoul National University, Korea, in 1991, 1993, and 1997, respectively. He has been with Chonbuk National University, Korea, since 1999. He is currently a professor at Chonbuk National University, Korea, and the director of the WeGAT Research Center, supported by the MSIP, Korea. He is also with the Smart Grid Research Center at Chonbuk National University. His research interests include the development of new protection and control systems for wind power plants and the enhancement of wind energy penetration levels.